available at www.sciencedirect.com

ScienceDirect

journal homepage: www.elsevier.com/locate/biochempharm

New structure model for the ATP-binding cassette multidrug transporter LmrA

Luca Federici [a,b], *Barbara Woebking* [c], *Saroj Velamakanni* [c], *Richard A. Shilling* [c], *Ben Luisi* [d], *Hendrik W. van Veen* [c,*]

[a] *Ce.S.I. Centro Studi sull'Invecchiamento, Fondazione Universita' "G. D'Annunzio", Via Colle dell'Ara, 66013 Chieti, Italy*
[b] *Dipartimento di Scienze Biomediche, Universita' di Chieti "G. D'Annunzio". Via Colle dell'Ara, 66013 Chieti, Italy*
[c] *Department of Pharmacology, University of Cambridge, Cambridge, UK*
[d] *Department of Biochemistry, University of Cambridge, Cambridge, UK*

ARTICLE INFO

Article history:
Received 26 March 2007
Accepted 21 May 2007

Keywords:
ABC transporter
Cysteine cross-linking
Homology modelling
LmrA
Multidrug resistance
Sav1866

ABSTRACT

Multidrug resistance of pathogenic microorganisms and mammalian tumors can be associated with the overexpression of multidrug transporters. These integral membrane proteins are capable of extruding a wide range of structurally unrelated compounds from the cell. Among the different classes of multidrug transporters are the ATP binding cassette (ABC) transporters, which are dependent on the binding and hydrolysis of ATP. In the past five years, many researchers have built homology models of ABC extrusion systems using the atomic coordinates of crystallized MsbA, a lipopolysaccharide transporter in Gram-negative bacteria. Likewise, we have previously used the *Vibrio cholera* MsbA structure as a template in the modeling of the multidrug transporter LmrA from *Lactococcus lactis*. In view of the recently discovered inaccuracies in the MsbA structure, we have remodelled LmrA using the atomic coordinates of the MsbA homologue Sav1866 from *Staphylococcus aureus*. To compare and test our MsbA-based and Sav1866-based LmrA models we performed cysteine cross-linking at three key positions in LmrA. The pattern of cross-linking at these positions was consistent with the overall topology of transmembrane helices in Sav1866, suggesting that its crystal structure might be physiologically relevant. We recently identified E314 as a residue important in proton conduction by LmrA. The predicted location of this residue at the interface between the two half-transporters in the Sav1866-based homodimer, within the inner leaflet of the phospholipid bilayer, provides a new structural basis for the role of E314 in LmrA-mediated transport.

1. Introduction

ATP-binding cassette (ABC) multidrug transporters are integral membrane proteins, which mediate the energy-dependent extrusion of structurally unrelated chemotherapeutic agents from the cell [1,2]. Their expression contributes to multidrug resistance in infectious diseases and cancer [3,4]. In addition, the activity of these systems affects the pharmacokinetics and pharmacodynamics of therapeutic drugs in mammals [3,4]. Knowledge about the structure and mechanisms of drug

* *Corresponding author at*: Department of Pharmacology, University of Cambridge, Tennis Court Road, CB2 1PD, United Kingdom. Tel.: +44 1223 765295; fax: +44 1223 334100.
E-mail address: hwv20@cam.ac.uk (H.W. van Veen).

Abbreviations: ABC, ATP-binding cassette; MD, membrane domain; NBD, nucleotide-binding domain; TMH, transmembrane helix

0006-2952/$ – see front matter
doi:10.1016/j.bcp.2007.05.015

recognition by multidrug transporters will facilitate the generation of new drugs, which can bypass drug pumping or inhibit drug pumping by the formation of a dead-end transporter-inhibitor complex [5].

ABC multidrug transporters usually contain four core domains. Two membrane domains (MDs) form the pathway for substrate translocation across the membrane. Drug transport by the MDs is thought to be driven by ATP-binding/hydrolysis at two nucleotide-binding domains (NBDs). The NBDs and MDs can be expressed in a multitude of arrangements [1]. The human multidrug resistance P-glycoprotein ABCB1 has the four core domains fused into a single polypeptide in an H_2N–(MD–NBD–MD–NBD)–COOH configuration [6]. LmrA from *L. lactis* [7], and other bacterial ''half-transporter'' homologues of ABCB1, including MsbA from *Escherichia coli* [8,9], BmrA from *Bacillus subtilis* [10], and Sav1866 from *S. aureus* [11,12] comprise an NH_2-terminal MD fused to one NBD. Recent studies established that, by analogy to the repeat of the LmrA-like half-transporter in ABCB1, the minimal unit in the functional LmrA transporter is the homodimer [13].

LmrA has been studied in intact lactococcal cells and membrane vesicles derived thereof, and in proteoliposomes containing purified and functionally reconstituted protein [13–15]. The protein has also been heterologously expressed in *E. coli* [7], *Spodoptera frugiperda* insect cells, and human lung fibroblast cells [16]. In each of these cases, LmrA has been shown to interact with a variety of drugs and modulators of ABCB1, making the bacterial protein a useful model for its mammalian counterpart and for homologues in pathogenic microorganisms. Insights into the structure of LmrA would allow detailed analyses of structure–function relationships in the transporter. Recently, high-resolution crystallographic structures were reported for Sav1866 [11,12], which differ substantially from the previously published crystallographic structures for MsbA [17,18]. Here, we describe a Sav1866-based homology model for LmrA, and we compare this model with our previous model based on *V. cholera* MsbA in a cysteine cross-linking approach.

2. Materials and methods

2.1. Molecular modelling of LmrA

To find a suitable alignment between the primary amino acid sequence of Sav1866 (PDB accession number 2HYD) and LmrA, two independent strategies were followed. In the first strategy, homologues of both LmrA and Sav1866 were searched using PHI-BLAST (http://www.ebi.ac.uk/), manually selected to represent both close and distant relatives, and were then aligned using Clustal-X. The second strategy made use of the recently developed automated Multiple Mapping Method (MMM) [19]. This method is regarded as being more accurate than simple alignment algorithms and it adopts the following protocol: inputs from five profile-to-profile based alignment methods are produced; the alternatively aligned regions from the different sets of alignments are then combined according to their fit in the structural environment of the template structure and a final alignment is produced. The alignments obtained by these two different procedures were compared, and were found to be substantially equivalent with some differences in the N-terminal region of the protein corresponding to transmembrane helix (TMH) 1 and TMH 2. The alignments were used to produce homology models with the program Modeller [20]. Ten models from each alignment were produced and the best one for each set was chosen based on the Modeller objective function which takes into account both energy and geometric violations. To assess which of the two procedures gave the best model, they were superimposed with the template structure. The model produced from the MMM alignment was perfectly superimposable on the Sav1866 template structure, with all the secondary structure elements topologically conserved and insertions or deletions restricted to loop regions. The model produced from the first procedure instead contained one insertion and one deletion in TMH 1 and 2, respectively; since these modifications break the helices in a region of the protein embedded in the membrane they were considered to be unlikely. Therefore, the model obtained from the MMM alignment was chosen (Fig. 1). The model was further validated using Procheck [21] and Verify3D [22]. The geometrical quality of the model is excellent, with 93.8% of residues lying in the most favored region of the Ramachandran plot, 5.8% in the additionally allowed region and only two residues out of 590 (0.4%) in the disallowed region. The electrostatic surface potential in Fig. 2 was calculated using Grasp [23].

2.2. Generation of LmrA mutants

Mutagenesis of (cysteine-less) wildtype *lmrA* was performed on plasmid pGHLmrA in *E. coli* [14] using the Quikchange kit (Stratagene, Amsterdam, The Netherlands) with primers 5′-GCA AGT TCC TAA G**TG C**GT TCA GCC-3′ and 5′-GGC TGA AC**G CA**C TTA GGA ACT TGC-3′ for M58C, 5′-GAC TCT TTA **TGT** AAT TTC CAA GGG -3′ and 5′-CCC TTG GAA ATT **ACA** TAA AGA GTC-3′ for A208C, and 5′-GGA ATC TA CTC ATA **TGC** ACG GGG GTT ATG AGT CTT GG-3′ and 5′-CCA AGA CTC ATA ACC CCC GT**G CA**T ATG AGA TAG ATT CC-3′ for S282C. The mutant *lmrA* genes were subcloned as NcoI-XbaI fragments in the lactococcal expression vector pNZ8048 [24,25], downstream of the *nisA* promoter, yielding pNHLmrA M58C, pNHLmrA A208C, and pNHLmrA S282C, respectively. The cloned PCR products were sequenced to ensure that only the intended changes were introduced.

2.3. Ethidium transport

L. lactis NZ9000 cells containing pNHLmrA plasmids were grown in M17 medium containing 0.5% glucose and 5 μg/ml chloramphenicol to an OD_{660} of 0.6. Protein expression was then induced for 1 h in the presence of nisin A (10 pg/ml) through the addition of 0.1% (v/v) of the culture supernatant of the nisin A-producing *L. lactis* strain NZ9700 [24]. The cells were harvested by centrifugation (4000 × *g*, 10 min, 4 °C), resuspended in an equal volume of assay buffer (50 mM KPi, pH 7.0, containing 5 mM $MgSO_4$), washed three times by centrifugation in the assay buffer, and diluted to an OD_{660} of 5. Preceding the ethidium transport measurements, the cells were diluted to an OD_{660} of 0.5 in assay buffer and preloaded

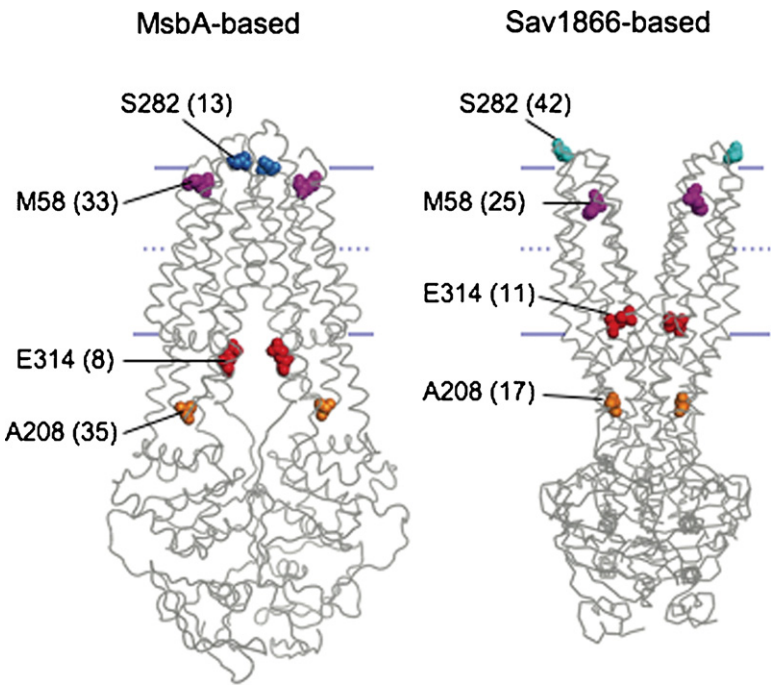

Fig. 1 – Homology models of LmrA based on *V. cholera* MsbA and Sav1866. Residues M58, A208 and S282 in LmrA were substituted by a cysteine for cross-linking studies, and are indicated in purple, orange and blue, respectively. E314 is indicated in red. Molecular distances (in Å) between these residues in one half-transporter and corresponding residues in the other half-transporter are indicated between brackets.

with 2 μM ethidium for about 40 min to a fluorescence level between 100 and 140 a.u. The ethidium fluorescence measurements were started, and after 30 s, the cells were allowed to generate metabolic energy by addition of 20 mM glucose. The ethidium fluorescence was followed as a function of time in a LS 55B fluorimeter (PerkinElmer Life and analytical sciences, UK) using excitation and emission wavelengths of 500 and 580 nm, respectively, and slit widths of 5 and 10 nm, respectively.

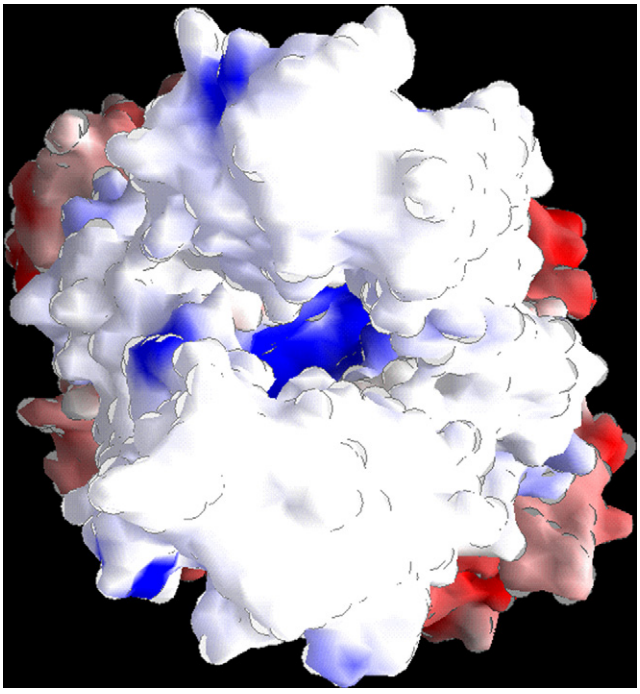

Fig. 2 – Electrostatic potential surface of the outward facing Sav1866-based LmrA model, viewed from the cell exterior. A positively charged extrusion chamber is visible (blue).

2.4. *Cross-linking*

Inside-out membrane vesicles containing wildtype (Wt) or mutant LmrA protein were diluted to 100 μg total membrane protein in 100 μl of 50 mM potassium phosphate buffer (pH 7.0). The cysteine-reactive crosslinker, 3,6,9,12,15-pentaoxaheptadecane-1,17-diyl-bis-methanethiosulfonate (Toronto research chemicals, Canada) was added from a stock of 50 mg/ml in dimethylsulfoxide to a final concentration of 0.5 mg/ml. After 10 min of incubation at 20 °C, the reaction was stopped by the addition of 10 mM *N*-ethylmaleimide. Samples were analyzed on western blot.

3. Results

3.1. *Modelling of LmrA using Sav1866 as a template*

LmrA and Sav1866 are closely related with an overall sequence identity of 30%. As a result the Sav1866-based model for LmrA (Fig. 1) is almost completely superimposable with the template Sav1866 structure with a root-mean-square-deviation of 0.615 Å for aligned Cα atoms. Such a low value indicates that it is possible to replace all Sav1866 side chains with the corresponding ones of LmrA, within the framework of the

same scaffold, and still obey the known rules of stereochemistry. Only two major differences in the protein scaffold are found. Firstly, a 22-residue long N-terminal extension is present in LmrA, which is lacking in Sav1866; this cytosolic extension was not modeled due to the absence of a reliable template. Secondly, the extracellular loop 1 (ECL1) between TMH 1 and TMH 2 is shorter by 11 residues in LmrA with respect to Sav1866. Apart from these differences, other insertions or deletions are limited to one or two residues in loop regions.

The Sav1866 protein was crystallized as a dimer with bound ADP [11] or AMP-PNP [12] with an outward-facing conformation of the MDs. In each of these structures the two NBDs are closely associated in the similar configuration adopted by the ATP-bound state of NBD dimers in BtuCD [26], MalK [27], MJ0796 [28], and the DNA repair protein Rad50 [29]. The nucleotide is engaged in a pocket formed by the P-loop of one NBD and the ABC signature of the other. The Sav1866 structure, and LmrA model derived from it, might therefore represent the ATP-bound state in which a drug extrusion chamber is open to the exterior of the membrane. This structure is thought to be consistent with the ATP-switch model for ABC transporters in which the conformational changes in the MDs required for transport are associated with changes in NBD: NBD interactions, which alternate between a closed dimeric conformation initiated by the binding of two molecules of ATP, and a nucleotide-free dimeric 'open' conformation [30,31].

The NBDs in the Sav1866-based LmrA model are interfaced to the MDs through noncovalent interactions with intracellular domains (ICDs), which are formed by cytosolic extensions of TMHs joined by two small helices in both ICD 1 and ICD 2. An analysis of the contacts between the MD of one monomer (residues 23–331) and the NBDs in both monomers (residues 332–590) was performed using the Contact Map Analysis tool of the Space server (http://ligin.weizmann.ac.il/cma/), imposing a threshold of 20 $Å^2$ for the contact surface among residues. This analysis showed that ICD 1 is mainly involved in contacting the NBD from the same monomer: three specific interactions were detected, the hydrogen bond H117-E333, the salt bridge K121-E332, and the hydrogen bond D124-Y399. A salt bridge interaction is also found involving K127 and E482 from the NBD of the other monomer. ICD 2 is instead mainly involved in contacting the NBD of the other monomer. Multiple interactions are present including the contacts S226-E396, S227-R503, K231-E419, and Q232-E448. A large chamber is formed by the MDs in the Sav1866-based LmrA model, which is exposed to the exterior of the cell, and which spans the outer and inner leaflets of the membrane but does not have access from the cytoplasm. The interior of the chamber in Sav1866-based LmrA is mainly lined by hydrophilic residues and, as in Sav1866, it is moderately positively charged (Fig. 2). This feature might be consistent with the notion that the outward-facing configuration of LmrA possesses a low affinity for hydrophobic cationic drugs [13].

3.2. *Experimental testing of the Sav1866-based LmrA model*

Single-cysteine replacements were introduced in the cysteine-less wildtype LmrA background at positions where their cross-linking could distinguish between the LmrA models based on the *V. cholera* MsbA and Sav1866 crystal dimers. Three cysteine mutants, M58C, A208C and S282C were generated, and each was expressed in *L. lactis* to the same level as wildtype LmrA. The functionality of the mutants was investigated in ethidium efflux measurements in cells preloaded with ethidium. In this transport assay, the extrusion of ethidium from the cell is determined from the decrease in the fluorescence of the intracellular ethidium-polynucleotide complex. As shown in Fig. 3, the A208C and S282C mutant proteins were equally active as wildtype LmrA. The extrusion of ethidium from cells expressing M58C LmrA was reduced compared to Wt LmrA, but remained significantly above the level in nonexpressing control cells. Hence, the single cysteine mutants were functional.

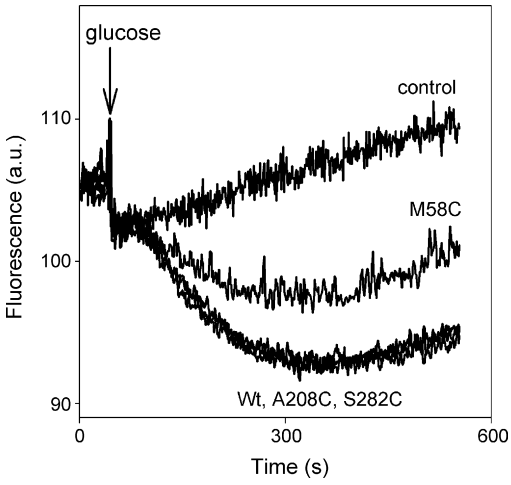

Fig. 3 – The single-cysteine mutants of LmrA mediate ethidium extrusion in *L. lactis*. For active ethidium efflux, control cells (control) or cells expressing LmrA (Wt) or mutant proteins (*M58C*, *A208C* or *S282C*) were preloaded for 40 min with 2 μM ethidium bromide. To allow the cells to generate metabolic energy, 20 mM glucose was added at 30 s after the fluorescence measurement was started. Ethidium transport was measured by fluorescence spectroscopy.

To assess the proximity of the introduced cysteine residues, we used a bifunctional cross-linker of approximately 25 Å in length exposing a thiol-reactive MTS group at either end (3,6,9,12,15-pentaoxaheptadecane-1,17-diyl-bis-methanethiosulfonate). As the functional dimer of LmrA is not covalently joined, any cross-linking of one LmrA half-transporter to the other will result in doubling the mass of the protein, which is easily observed using SDS-PAGE. The cysteine cross-linking was performed in inside-out membrane vesicles, with the protein in its native lipid environment (Fig. 4). To ensure that the signals revealed by western blot analysis against the His_6-tagged LmrA were due to the cysteine cross-linking, samples were run with and without reduction of disulphide bonds with β-mercaptoethanol. Cysteine-replacement S282C in one half-transporter was predicted to be close enough to S282C in the other half-transporter for a crosslink in *V. cholera*-MsbA-based LmrA model but not in the Sav1866-based LmrA model (Fig. 1). In cross-

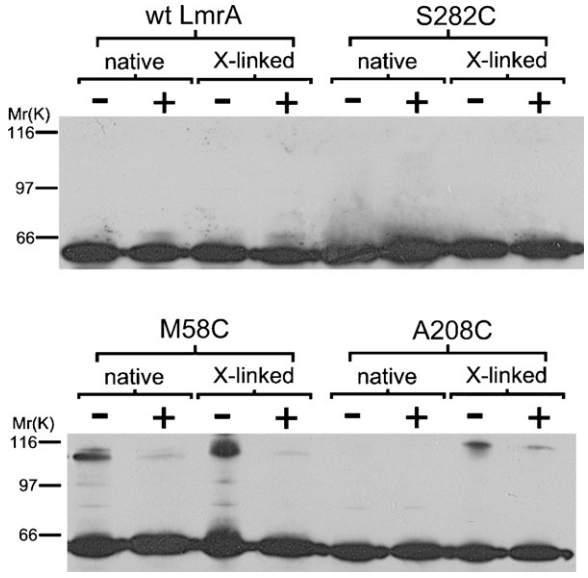

Fig. 4 – Cross-linking of single-cysteine mutants of LmrA. Wt and mutant LmrA proteins in inside-out membrane vesicles were incubated in the absence (native) or presence (X-linked) of the bis-methanethiosulfonate cross-linker. Samples were treated without (−) or with (+) the reducing agent β-mercaptoethanol to test that cross-linking was based on disulphide bond formation. Total membrane proteins were separated by 10% SDS-PAGE and analysed on immunoblot.

linking experiments, this mutant failed to show bands higher than the monomer (Fig. 4). On the other hand, cysteine replacements M58C and A208C were predicted to be located at positions in the Sav1866-based homodimer where the thiol moieties were accessible and close enough for cross-linking (Fig. 4). The residues would be unavailable for cross-linking in the VC-MsbA-based homodimer due to the physical obstruction of these residues by TMHs. In cross-linking experiments, clear β-mercaptoethanol-sensitive signals were obtained for the M58C and A208C mutants, each with a molecular mass twice that of LmrA (Fig. 4). The M58 mutant formed the dimer even in the absence of cross-linker, which might explain the reduced ethidium transport activity of this mutant compared to Wt LmrA and the A208C and S282C mutants (Fig. 4). The cross-linking of the M58C mutant suggests that a conformation must exist for dimeric LmrA in which both M58 residues are very close; this observation is incompatible with *V. cholera*-MsbA-based LmrA, where the M58C residues are unable to react due to their predicted position at the external face of the MDs. Taken together, the cross-linking data obtained for the single-cysteine mutants are consistent with the notion that the predicted orientations of the MD of LmrA might reflect a physiologically relevant state.

4. Discussion

In 2001 and following years, the first X-ray structures became available for MsbA from *E. coli*, *V. cholera* and *Salmonella typhimurium*, based on diffraction data at 4.5, 3.8 and 4.2 Å resolution, respectively [17]. In each of these cases, the experimental electron density maps suggested that MsbA crystallizes as a dimer, and that, consistent with the crystal structure of the vitamin B12 uptake system BtuCD from *E. coli* [26], the MD of MsbA is composed of transmembrane α-helices which are extended intracellularly in ICDs that form the interface with the NBD. However, when compared with each other, the MsbA structures exhibited unexpected and very different quaternary arrangements. In spite of these discrepancies, the *E. coli* MsbA and *V. cholera*-MsbA structures were used as a starting point for the generation of homology models of ABCB1 [32–35], the human multidrug resistance protein MRP1 (ABCC1) [36], and bacterial MsbA [37], BmrA [38], and LmrA [39]. In many of these models, the NBDs were replaced and/or rearranged to resemble the dimeric NBD: NBD interface observed in the BtuCD, MalK, Rad50 and MJ0796 structures [26–29]. In the case of the ABCB1 model by Stenham et al. [32] this rearrangement also involved a rotation of the MDs towards each other, which then form a central pore open to the exterior. As the structures of the MD of the *E. coli*, *V. cholera* and *S. typhimurium* MsbA monomers were all in agreement with each other, we previously generated a *V. cholera*-MsbA-based homology model of a truncated LmrA protein comprising solely the MD in the absence of the NBD (LmrA-MD) to avoid the confusion regarding NBD structure and orientation [14].

The recently determined crystal structures of the ABC transporter Sav1866 from *S. aureus* at 3.0 [11] and 3.4 Å resolutions, respectively, [12] are different from the reported MsbA crystal structures [17]. A comparison of Sav1866 and MsbA structures suggested that the Cα backbone of MsbA was built on incorrectly calculated electron density maps resulting in an incorrect protein topology. As a result of this, Chang et al. recently retracted the publications describing the MsbA structures [18]. The availability of the Sav1866 structures prompted us to remodel LmrA, and compare the new Sav1866-based LmrA model with our previous MsbA-based model in a cysteine cross-linking approach in which cysteine replacements were chosen at key positions that would discriminate between both models. The introduction of the cysteine replacements did not alter the gross structure of LmrA, as the mutant proteins were all transport-active in the ethidium efflux assay (Fig. 3). The observations on the occurrence of cross-linking for the M58C and A208C mutants, but not for the S282C mutant, are consistent with the predictions made by the Sav1866-based model (Figs. 1 and 4). It is interesting to note that our new LmrA model is based on the crystal structure of a Sav1866 dimer that presumably is in the ATP-bound state, whereas our cross-linking studies were performed in the absence of the nucleotide. However, we have previously shown that conformational changes in the MD of LmrA required for transport are reversible and can occur in the absence of ATP-binding/hydrolysis [14,40].

In our previous modeling of LmrA based on the *V. cholera*-MsbA template, we identified E314 as a residue located in the cytosolic extension of TMH 6 (termed ICD 3) and putatively positioned in the drug-binding chamber at the cytosol-membrane interface [14] (Fig. 1). An E314A replacement affected the maximum rate of ethidium efflux rather than

the affinity for ethidium, which implicated this residue in a mechanistic role rather than in direct interactions with the ligand. These data were rationalized by the observation that the LmrA-mediated cotransport of ethidium and protons can be driven by transmembrane potential and transmembrane chemical proton gradient (ΔpH) [15]. The E314A mutant abolishes the dependence of this reaction on the ΔpH suggesting a role of E314 in proton binding.

It is interesting to note that the positions of E314 in the *V. cholera*-MsbA-based and Sav1866-based models share some similarity; E314 is facing the central chamber between the two half-transporters in each of these models (Fig. 1). However, the models differ in the details. In the *V. cholera*-MsbA model, E314 was predicted to be located at cytoplasmic side of the interface between cytosol and inner membrane leaflet [14]. In contrast, the residue is located within the inner leaflet in the Sav1866-based model. E314 was also predicted to have a relatively high pKa resulting in its protonation in an inward-facing state of the transporter, potentially due to neighboring hydrophobic residues [14]. The release of the bound proton from E314 in the outward-facing conformation would be facilitated if the surrounding residues were hydrophilic in this state. Consistent with this suggestion, our new Sav1866-based model predicts that E314 is embedded by the polar side chains of N144, N148, T310, and T313; thus, E314 might be deprotonated in this outward-facing conformation (Fig. 5).

In conclusion, we have remodeled LmrA using the atomic coordinates of the Sav1866 crystal dimer. Our cysteine cross-linking experiments for LmrA support the overall topology of TMHs predicted by the Sav1866 structure. Consistent with the functional role of E314 in proton-dependent ethidium transport, both half-transporters in the Sav1866-based LmrA dimer are predicted to expose E314 at a strategic location, at their interface within the inner leaflet of the membrane.

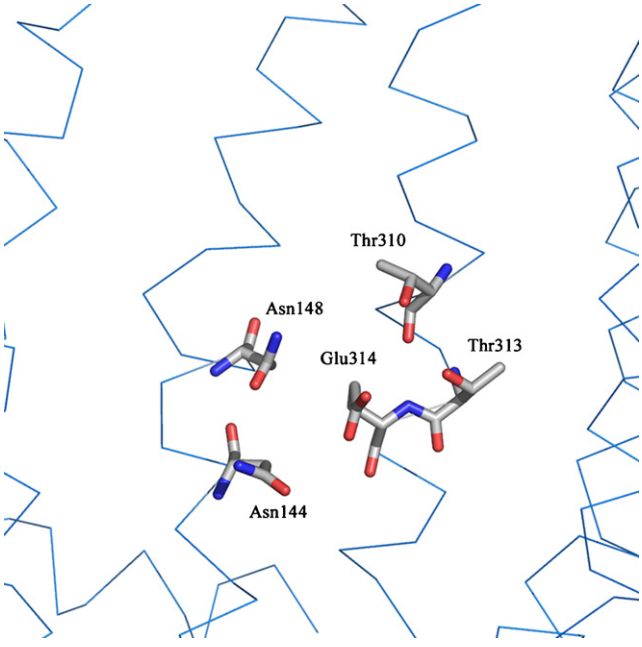

Fig. 5 – E314 is predicted to be located in TMH 6 of LmrA, inside the exposed chamber between the two half-transporters, and close to the inner leaflet of the membrane. The proximal residues are also shown and define a markedly hydrophilic surrounding for E314 in this protein conformation.

Acknowledgments

We thank Kaspar Locher for sharing the coordinates of the Sav1866 structure prior to publication. We also appreciate discussions with Geoffrey Chang. This work was supported by the Biotechnology and biological sciences research council (BBSRC) and Welcome trust.

REFERENCES

[1] Higgins CF. Multiple molecular mechanisms for multidrug resistance transporters. Nature 2007;446:749–57.
[2] Jones PM, George AM. The ABC transporter structure and mechanism: perspectives on recent research. Cell Mol Life Sci 2004;61:682–99.
[3] Borst P, Elferink RO. Mammalian ABC transporters in health and disease. Annu Rev Biochem 2002;71:537–92.
[4] Hardwick LJA, Velamakanni S, van Veen HW. The emerging significance of the breast cancer resistance protein (ABCG2). Br J Pharmacol 2007;151:163–74.
[5] Shilling RA, Venter H, Velamakanni S, Bapna A, Woebking B, Shahi S, et al. New light on multidrug binding by an ATP-binding-cassette transporter. Trends Pharmacol Sci 2006;27:195–203.
[6] Sharom FJ. Shedding light on drug transport: structure and function of the P-glycoprotein multidrug transporter (ABCB1). Biochem Cell Biol 2006;84:979–92.
[7] van Veen HW, Venema K, Bolhuis H, Oussenko I, Kok J, Poolman B, et al. Multidrug resistance mediated by a bacterial homologue of the human multidrug transporter MDR1. Proc Natl Acad Sci USA 1996;93:10668–72.
[8] Woebking B, Reuter G, Shilling RA, Velamakanni S, Shahi S, Venter H, et al. Drug-lipid A interactions on the *Escherichia coli* ABC transporter MsbA. J Bacteriol 2005;187:6363–9.
[9] Doerrler WT. Lipid trafficking to the outer membrane of Gram-negative bacteria. Mol Microbiol 2006;60:542–52.
[10] Steinfels E, Orelle C, Fantino JR, Dalmas O, Rigaud JL, Denizot F, et al. Characterization of YvcC (BmrA), a multidrug ABC transporter constitutively expressed in *Bacillus subtilis*. Biochemistry 2004;43:7491–502.
[11] Dawson RJ, Locher KP. Structure of a bacterial multidrug ABC transporter. Nature 2006;443:180–5.
[12] Dawson RJ, Locher KP. Structure of the multidrug ABC transporter Sav1866 from *Staphylococcus aureus* in complex with AMP-PNP. FEBS Lett 2007;581:935–8.
[13] Van Veen HW, Margolles A, Muller M, Higgins CF, Konings WN. The homodimeric ATP-binding cassette transporter LmrA mediates multidrug transport by an alternating two-site (two-cylinder engine) mechanism. EMBO J 2000;19:2503–14.
[14] Shilling R, Federici L, Walas F, Venter H, Velamakanni S, Woebking B, et al. A critical role of a carboxylate in proton conduction by the ATP-binding cassette multidrug transporter LmrA. FASEB J 2005;19:1698–700.
[15] Venter H, Shilling RA, Velamakanni S, Balakrishnan L, Van Veen HW. An ABC transporter with a secondary-active multidrug translocator domain. Nature 2003;426:866–70.
[16] Van Veen HW, Callaghan R, Soceneantu L, Sardini A, Konings WN, Higgins CF. A bacterial antibiotic-resistance

gene that complements the human multidrug-resistance P-glycoprotein gene. Nature 1998;391:291–5.
[17] Reyes CL, Ward A, Yu J, Chang G. The structures of MsbA: insight into ABC transporter-mediated multidrug efflux. FEBS Lett 2006;580:1042–8.
[18] Chang G, Roth CB, Reyes CL, Pornillos O, Chen YJ, Chen AP. Retraction. Science 2006;314:1875.
[19] Rai BK, Madrid-Aliste CJ, Fajardo JE, Fiser A. MMM: a sequence-to-structure alignment protocol. Bioinformatics 2006;22:2691–2.
[20] Sali A, Blundell TL. Comparative protein modeling by satisfaction of spatial restraints. J Mol Biol 1993;234: 779–815.
[21] Laskowski RA, Moss DS, Thornton JM. Main-chain bond lengths and bond angles in protein structures. J Mol Biol 1993;231:1049–67.
[22] Eisenberg D, Luthy R, Bowie LU. Verify3D: assessment of protein models with three-dimensional profiles. Methods Enzymol 1997;277:396–404.
[23] Nicholls A, Sharp KA, Honig B. Protein folding and association: insights from the interfacial and thermodynamic properties of hydrocarbons. Proteins 1991;11:281–96.
[24] De Ruyter PG, Kuipers OP, De Vos WM. Controlled gene expression for *Lactococcus lactis* with the food-grade inducer nisin. Appl Environ Microbiol 1996;62:3662–7.
[25] Margolles A, Putman M, Van Veen HW, Konings WN. The purified and functionally reconstituted multidrug transporter LmrA of *Lactococcus lactis* mediates the transbilayer movement of specific fluorescent phospholipids. Biochemistry 1999;38:16298–306.
[26] Locher KP, Lee AT, Rees DC. The *Escherichia coli* BtuCD structure: a framework for ABC transporter architecture and mechanism. Science 2002;296:1091–8.
[27] Chen J, Lu G, Lin J, Davidson AL, Quiocho FA. A tweezers-like motion of the ATP-binding cassette dimer in an ABC transport cycle. Mol Cell 2003;12:651–61.
[28] Smith PC, Karpowich N, Millen L, Moody JE, Rosen J, Thomas PJ, et al. ATP binding to the motor domain from an ABC transporter drives formation of a nucleotide sandwich dimer. Mol Cell 2002;10:139–49.
[29] Hopfner KP, Karcher A, Shin DS, Craig L, Arthur LM, Carney JP, et al. Structural biology of Rad50 ATPase: ATP-driven conformational control in DNA double-strand break repair and the ABC-ATPase superfamily. Cell 2000;101:789–800.
[30] Higgins CF, Linton KJ. The ATP switch of ABC transporters. Nat Struct Mol Biol 2004;11:918–26.
[31] Sauna ZE, Ambudkar SV. About a switch: how P-glycoprotein (ABCB1) harnesses the energy of ATP binding and hydrolysis to do mechanical work. Mol Cancer Ther 2007;6:13–23.
[32] Stenham DR, Campbell JD, Sansom MS, Higgins CF, Kerr ID, Linton KJ. An atomic detail model for the human ATP binding cassette transporter P-glycoprotein derived from disulfide cross-linking and homology modeling. FASEB J 2003;17:2287–9.
[33] Seigneuret M, Garnier-Suillerot A. A structural model for the open conformation of the mdr1 P-glycoprotein based on the MsbA crystal structure. J Biol Chem 2003;278:30115–24.
[34] Pleban K, Kopp S, Csaszar E, Peer M, Hrebicek T, Rizzi A, et al. P-glycoprotein substrate binding domains are located at the transmembrane domain/transmembrane domain interfaces: a combined photo affinity labeling-protein homology modeling approach. Mol Pharmacol 2005;67: 365–74.
[35] Al-Shawi MK, Omote H. The remarkable transport mechanism of P-glycoprotein: a multidrug transporter. J Bioenerg Biomembr 2005;37:489–96.
[36] Campbell JD, Koike K, Moreau C, Sansom MS, Deeley RG, Cole SP. Molecular modeling correctly predicts the functional importance of Phe594 in transmembrane helix 11 of the multidrug resistance protein. MRP1 (ABCC1). J Biol Chem 2004;279:463–8.
[37] Campbell JD, Biggin PC, Baaden M, Sansom MS. Extending the structure of an ABC transporter to atomic resolution: modeling and simulation studies of MsbA. Biochemistry 2003;42:3666–73.
[38] Dalmas O, Orelle C, Foucher AE, Geourjon C, Crouzy S, Di Pietro A, et al. The Q-loop disengages from the first intracellular loop during the catalytic cycle of the multidrug ABC transporter BmrA. J Biol Chem 2005;280:36857–64.
[39] Ecker GF, Pleban K, Kopp S, Csaszar E, Poelarends GJ, Putman M, et al. A three-dimensional model for the substrate binding domain of the multidrug ATP binding cassette transporter LmrA. Mol Pharmacol 2004;66:1169–79.
[40] Balakrishnan L, Venter H, Shilling RA, Van Veen HW. Reversible transport by the ATP-binding cassette multidrug export pump LmrA: ATP synthesis at the expense of downhill ethidium uptake. J Biol Chem 2004;279:11273–80.